water

MDPI

Article

Simulation and Optimisation Using a Digital Twin for Resilience-Based Management of Confined Aquifers

Carlos Segundo Cohen-Manrique [1,*], José Luis Villa-Ramírez [2], Sergio Camacho-León [3], Yady Tatiana Solano-Correa [2], Alex A. Alvarez-Month [4] and Oscar E. Coronado-Hernández [5]

[1] Facultad de Ciencias Básicas, Ingeniería y Arquitectura, Corporación Universitaria del Caribe-CECAR, Sincelejo 763022, Colombia
[2] Grupo de Investigación en Física Aplicada y Procesamiento de Imágenes y Señales (FAPIS), Universidad Tecnologica de Bolivar—UTB, Cartagena de Indias 130001, Colombia; jvilla@utb.edu.co (J.L.V.-R.); solanoy@utb.edu.co (Y.T.S.-C.)
[3] Tecnologico de Monterrey, School of Engineering and Sciences, Monterrey 64849, Mexico; sergio.camacho@tec.mx
[4] Facultad de Ingeniería, Universidad de Sucre, Sincelejo 700001, Colombia; alex.alvarez@unisucre.edu.co
[5] Instituto de Hidráulica y Saneamiento Ambiental, Universidad de Cartagena, Cartagena 130001, Colombia; ocoronadoh@unicartagena.edu.co
* Correspondence: carlos.cohen@cecar.edu.co or ccohen@utb.edu.co

Abstract

Efficient management of groundwater resources is essential for environmental sustainability. This study introduces the development and application of a digital twin (DT) for confined aquifers to optimise water extraction and ensure long-term sustainability. A resilience-based control model was implemented to manage the Morroa Aquifer (Colombia). This model integrated historical, hydrogeological, and climatic data acquired from in-situ sensors and satellite remote sensing. Several heuristic methods were employed to optimise the parameters of the objective function, which focused on managing water extraction in aquifer wells: grid search, genetic algorithms (GA), and particle swarm optimisation (PSO). The results indicated that the PSO algorithm yielded the lowest root mean square error (RMSE), achieving an optimal extraction rate of 8.3 l/s to maintain a target dynamic water level of 58.5 m. Furthermore, the model demonstrated the unsustainability of current extraction rates, even under high-rainfall conditions, highlighting the necessity for revising existing water extraction strategies to safeguard aquifer sustainability. To showcase its practical functionality, a DT prototype was deployed in a well within the Morroa piezometric network (Sucre, Colombia). This prototype utilised an ESP32 microcontroller and various sensors (DS18B20, SKU-SEN0161, SKU-DFR0300, SEN0237-A) to monitor water level, pH, dissolved oxygen, and temperature. The implementation of this DT proved to be a crucial tool for the efficient management of water resources. The proposed methodology provided key information to support decision-making by environmental management entities, thereby optimising monitoring and control processes.

Keywords: digital twin; resiliency; sensors; LULC; remote sensing; groundwater; control

Academic Editors: Yuntao Wang and Xiaoli Zhang

Received: 19 April 2025
Revised: 19 June 2025
Accepted: 25 June 2025
Published: 30 June 2025

Citation: Cohen-Manrique, C.S.; Villa-Ramírez, J.L.; Camacho-León, S.; Solano-Correa, Y.T.; Alvarez-Month, A.A.; Coronado-Hernández, O.E. Simulation and Optimisation Using a Digital Twin for Resilience-Based Management of Confined Aquifers. *Water* **2025**, *17*, 1973. https://doi.org/10.3390/w17131973

1. Introduction

Water is one of the planet's most crucial resources, and life on Earth depends on it profoundly. Therefore, global efforts encompassing economic, educational, research, and political initiatives have been developed to ensure its conservation, making it a Sustainable Development Goal (SDG 6: Clean Water and Sanitation). This issue transcends race,

creed, and economic systems, as both industrialised and developing nations increasingly need to invest in conserving and preserving water sources [1]. Fortunately, technological advancements in hardware and software capabilities have refined technologies such as remote sensing and hydrological science. These advancements have enabled the discovery of large underground water reserves worldwide, particularly in regions historically lacking this resource, such as sub-Saharan Africa, the Sahel region, and the Great Artesian Basin in Australia [2]. Additionally, crises resulting from overexploitation and depletion stress have been assessed in many of the world's largest reservoirs [3], such as the Arabian aquifer system, the Indus Basin aquifer in northwest India and Pakistan, and California's Central Valley. Despite these advancements, water remains one of the resources least valued by the global population [4]. In addition to the water stress caused by overexploitation and the rapid increase in the worldwide population [5], the high level of pollution to which water is subjected daily, whether from industry or the tons of waste generated in human settlements, must also be considered [6].

This research presents the results of a digital twin (DT) focused on optimising water resources in the Morroa Aquifer, Colombia. This confined aquifer, vital for communities in the central-western Caribbean region of Colombia for decades, has faced significant challenges due to population growth, potential contamination from agricultural and livestock practices, and inadequate water resource management. These factors have significantly increased the stress and burden on the aquifer, resulting in profound implications for its capacity, particularly its water levels (both static and dynamic ones). Consequently, it has become the second most overexploited aquifer globally, with worrying repercussions for future generations [7].

To maintain an innovative approach, the proposal integrates hydrogeological models, remote sensing, embedded systems, low-power data transmission, advanced control, and machine learning to improve analysis and decision-making in water resource management. To address this, a comprehensive review of the literature was conducted across several databases, such as Scopus, IEEE Xplore and Web of Science, prioritising topics related to the implementation of DT, resilience, remote sensing, land use and land cover (LULC), and optimal or predictive control in confined aquifers. Several authors have proposed conceptual models related to aquifers and their resilience-based management. For instance, ref. [8] implemented an aquifer resilience model that contributed to the sustainable management of groundwater by using a case study based in Denmark. This model focused on identifying key variables that described both quantitative and qualitative responses of the groundwater flow system to pumping, thus achieving a comprehensive approach. However, its effectiveness heavily depended on the quality of in situ data and presented high complexity in its implementation, which may limit its applicability in aquifers with insufficient monitoring. Other researchers have focused their attention on developing conceptual models of groundwater flow using hydrogeological, numerical, hydrochemical, and isotopic approaches [9–12]. Meanwhile, ref. [13] developed a conceptual groundwater model that includes interactions with surface waters for drought-sensitive areas, although it does not apply to confined aquifers. In remote sensing, ref. [14] used satellite imagery to model changes in land cover and their influence on land surface temperature (LST). Vegetation was determined to be the primary factor in surface overheating, whereas water bodies played a significant role in regulating LST. In contrast, areas with bare soil and built-up infrastructure contributed to the elevated levels of this variable. Ref. [15] utilised Sentinel-2 data, Normalised Difference Vegetation Index (NDVI), and multiple regression methods to examine the impacts of climatic factors such as humidity, precipitation, and air temperature on vegetation dynamics from 2015 to 2021 in Dhofar, Oman. They used a random forest regression algorithm to model the relationships between NDVI and variables

such as temperature, humidity, rainfall, soil maps, geological maps, topographic wetness index, curvature, elevation, slope, aspect, and distance to buildings and roads. Multiple regression values revealed significant associations between the spatial distributions of NDVI and the aforementioned climatic factors. Ref. [16] developed a model predictive control (MPC) system that considers the dynamic variation in water demand, precipitation, climate, and seasonal changes in electricity prices to manage water resources in Zahedan, Iran. However, their model focused on controlling distribution networks rather than optimising groundwater resources. As an example of the interaction between different areas related to water resources, ref. [17] proposed an intelligent water grid (SWG) with DT for the water infrastructure to improve the system's monitoring, management, and efficiency. This tool enables real-time monitoring of system components and analyses various scenarios and variables, such as pressure, operational devices, valve regulation, and head loss factors. In addition, the authors conducted a case study on the island of Madeira, Portugal, where local constraints exacerbate significant water losses.

The reviewed literature on DT highlights their rapid expansion in the water, environmental, and energy sectors. This growth is driven mainly by their ability to integrate and analyse multidisciplinary data, which has facilitated their widespread adoption, particularly in industrial sectors related to water management [18]. Key applications include the real-time monitoring and optimisation of drinking water and wastewater treatment plants [19], efficient management of water supply systems [20], and the development of smart urban aqueducts [21]. Furthermore, DT has been proven valuable in sustainable water governance systems [22] and in disaster risk reduction using advanced predictive simulations [23]. Furthermore, more specialised applications have been identified, such as monitoring pumps in deep aquifers [24] and tracking groundwater table levels [25]. These examples highlight the versatility and potential of this technology in various hydrological contexts.

Most research has focused on conceptual hydrogeological models to manage contamination and water resource consumption, using various tools focused on specific areas [26,27]. However, no models have been identified that integrate alternatives, such as optimal or predictive control, remote sensing tools, the Internet of Things, and hydrogeological models to manage groundwater aquifers with low resilience over time. Therefore, this work aims to propose a multidisciplinary strategy aimed at the resilient management of one of the most overexploited confined aquifers in the world, the Morroa Aquifer in Colombia, which faces a high risk of disappearing in the medium term. This creates significant difficulties for populations that depend directly or indirectly on their resources [7].

2. Materials and Methods

2.1. Study Area

The region of interest (ROI) is located in the Caribbean region of Colombia, encompassing the departments of Córdoba, Sucre, and Bolívar. From a geospatial perspective, the Morroa Aquifer is located in the border region between the departments of Sucre and Córdoba Figure 1. It spans approximately 9000 km^2, with a surface area of roughly 650 km^2, stretching from Ovejas (Sucre) to Chinú (Córdoba). This area features a topography that varies from steep hills in Ovejas to gentler, undulating terrain towards the south, gradually flattening out near Sampués. Geographically situated in northwestern Colombia, the climate alternates between humid and dry, with vegetation including secondary forests, small remnants of primary forests, shrublands and extensive grasslands. According to Holdridge's classification [28], the area is classified as a tropical dry forest (bs-T), part of the azonal lowland biome system (Savanna Pedobiome), with Isomegathermic climatic formations [29]. The average temperature in the region is 28 °C, and annual precipitation

ranges from 1000 to 1200 mm, with considerable sporadic variations related to natural climatic phenomena, such as La Niña or El Niño.

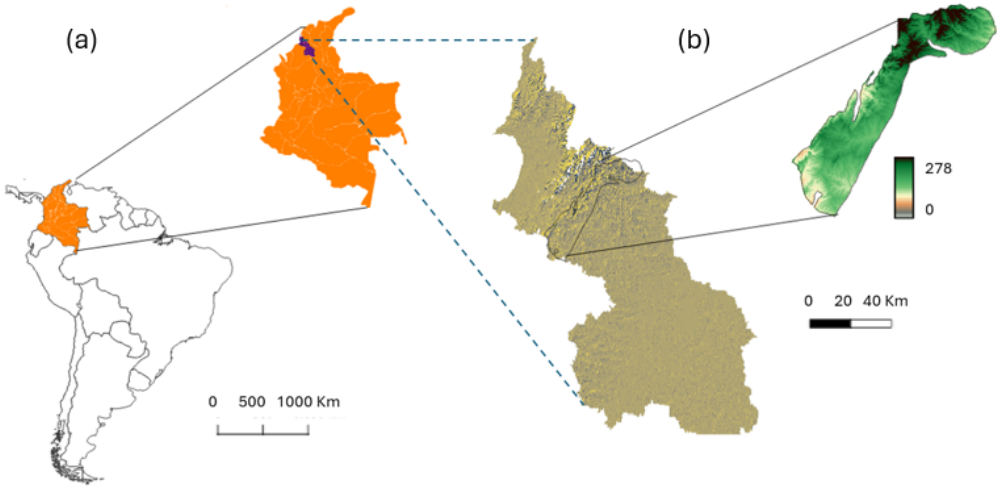

Figure 1. (**a**) Location of the ROI, (**b**) Digital Elevation Model of the department of Sucre (Colombia) and the ROI.

Figure 2 shows the precipitation patterns over 34 years for the central and most populated municipalities within the aquifer coverage area, which almost entirely depend on this water resource for potable water consumption. However, considering that evapotranspiration (ET) constitutes a crucial part of the terrestrial hydrological cycle [30], it is regarded as the primary cause of water loss on continental surfaces [31]. Generally, its rate increases in response to rising temperatures, wind speeds, and solar radiation. Given its significance, ET has been widely used in managing droughts, floods, and agriculture. Therefore, the FAO, numerous organisations, researchers, and soil and water resources experts consider it a fundamental variable in hydrological cycle modelling [6].

Figure 2 (right) shows the Penman–Monteith–Leuning (PML) evapotranspiration (ET) in the region of interest (ROI) from 2000 to 2022, generated using the Google Earth Engine (GEE) with JavaScript algorithms that assessed the median composite of the obtained data [32,33].

It is important to note that PML is divided into vegetation transpiration (blue line, Ec), which refers to the amount of water lost by vegetation due to heat, radiation, or temperature; direct soil evaporation (red line, Es); and vaporisation of intercepted rain by vegetation (orange line, Ei). Evaluating this PML is crucial, as it provides insights into the characteristics of the vegetation on the surface of the aquifer and its direct relationship with water consumption.

Both the rainfall and evapotranspiration levels shown in Figure 2 reveal two distinct seasons in the study area. The rainy season, extending from April to September or October, is characterised by frequent and occasional torrential rains. The dry season, covering the months from October to November to March and April, experiences high levels of solar radiation and significantly increases the soil aridity. This is clearly illustrated in Figure 3a, which presents a comparative analysis between two images from the European Space Agency (ESA) Sentinel-2 satellite for September 2023 and January 2024, with a spatial resolution of 10 m per pixel. These images are used to calculate the Normalised Difference Vegetation Index (NDVI), which is directly related to the difference between the high absorption of solar radiation by plants in the red band (owing to chlorophyll) and the high reflection of radiation in the near-infrared band (owing to their structure and water

content) [34]. Thus, NDVI is a good indicator of vegetation's greenness (photosynthesis or productivity) and its health status [35]. Observing the comparison, the change in vegetation cover recorded in both satellite images was evident. In the image on the left (September), the vegetation cover is predominantly classified as Medium and High Vegetation due to the lush and vibrant landscape resulting from rain.

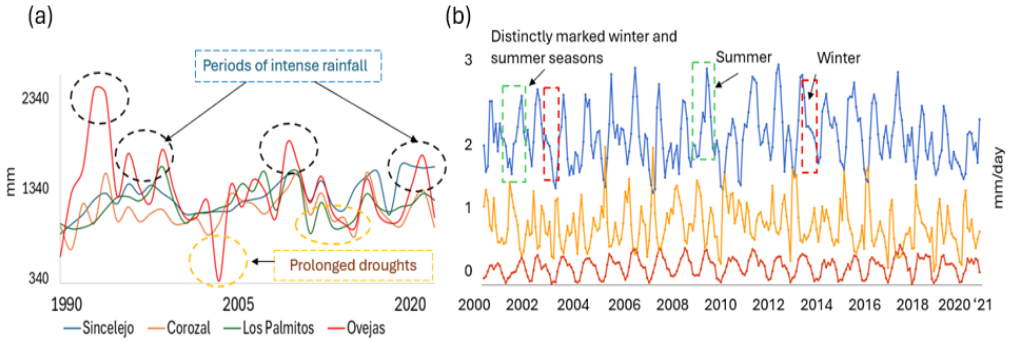

Figure 2. (**a**) Annual precipitation values in the five main settlements within the Morroa aquifer area [29]. (**b**) Behaviour of PML in the study area, divided into vegetation transpiration (Ec), direct soil evaporation (Es), and vaporisation of rain intercepted by vegetation (Ei).

In contrast, the image on the right (January) depicts the situation captured by the satellite during the dry season, where the vegetation cover changes substantially with low values of the prevailing vegetation index. This is due to the high temperatures and solar radiation recorded in the study area during the summer months, which increased soil dryness, resulting in less healthy and less dense vegetation that is less conducive to water capture for aquifer recharge. This indicates that the study area behaves as a semi-arid region during this time of the year.

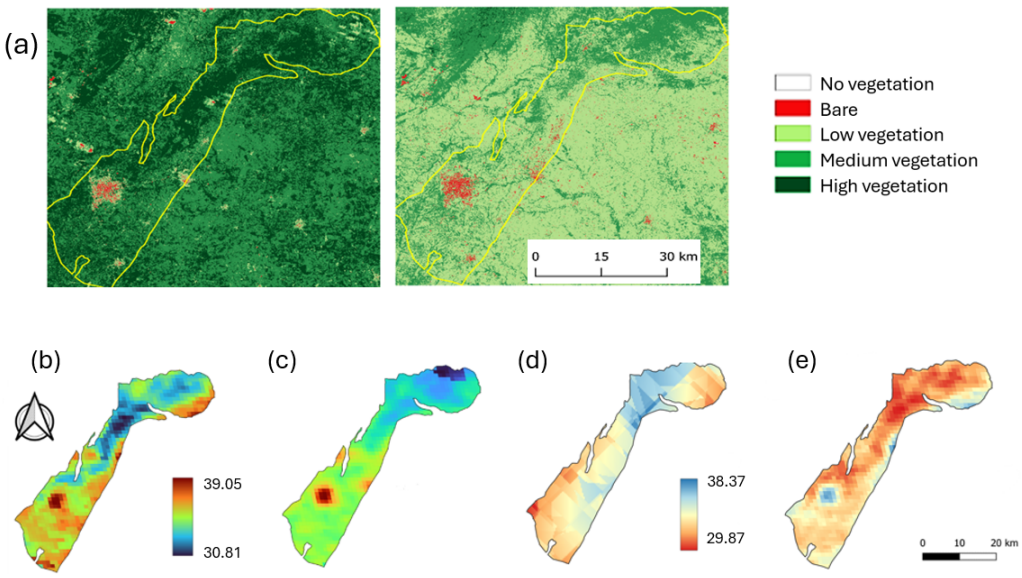

Figure 3. (**a**) Comparison of the NDVI index in the area adjacent to the study site during the wet season (September 2023) and the dry season (January 2024). Monthly variation of land surface temperature (LST) in degrees Celsius (**b**,**c**), and precipitation in mm/month (**d**,**e**) during the same seasons.

As an additional element to understand the study area, and considering that temperature and topography have notable impacts on the hydrological cycle [36], Figure 3b–e includes land surface temperature (LST) maps for the area of interest for February (Figure 3b) and November 2023 (Figure 3c). These data were obtained from NASA's Moderate Resolu-

tion Imaging Spectroradiometer (MODIS) [37]. The ROI is characterised by a multi-annual average temperature of approximately 28.15 °C. In the central zone (cities of Sincelejo, Morroa, and Corozal) and in the municipalities of Ovejas, Chalán, and the northern part of Colosó, the lowest temperatures were recorded, averaging approximately 27 °C. This situation is fundamentally associated with the elevation of this area, where heights of up to 686 m above sea level are found, as shown in Figure 1. Additionally, the spatial distribution of precipitation during the summer (January, Figure 3d) and winter (September, Figure 3e) of 2023 was observed using the heat map. Considering that the rainfall regime of the Sucre Department is unimodal with a dry period starting at the end of October, decreasing during December, and being extremely dry during January, February, and March, in April, some rain fell, which became widespread from May onwards. In July, there was a slight decrease called "veranillo"; the cycle ended in September and October, with the highest precipitation concentration. In these two months, more water fell than the average amount of the five dry months contributed from December to April [38].

2.2. Data Collection

The data collection used for precipitation in the region of interest employed to feed the proposed DT model was obtained from the Institute of Hydrology, Meteorology, and Environmental Studies (IDEAM) (www.ideam.gov.co). For evapotranspiration PML, NASA's Global Land Data Assimilation System Version 2.1 (GLDAS-2.1) was used with MODIS images (MODIS/NTSG/MOD16A2/105), making use of a 500 m spatial resolution per pixel and an 8-day satellite transit frequency. Temperature (LST) and precipitation maps in the ROI were obtained from NASA's Moderate Resolution Imaging Spectroradiometer (MODIS) satellite (MOD11A1.061) Daily Global Terra Land Surface Temperature and Emissivity, with a spatial resolution of 1 km on a 1200 × 1200 km grid. The in situ data were provided by Carsucre, who recorded aquifer level data through field brigades for over 30 years. The provided data included variables such as static level, dynamic level, desired level in wells, water extraction volume, and parameters related to water quality (pH, conductivity, etc.). Owing to the lack of technological tools, sensors, and control systems that record data in real time, measurements were conducted monthly and, in some cases, bimonthly. In addition, these measurements exhibited issues with noise, outliers, and frequently missing data. Information on soil types within the study area, historical land use parameters, and orographic data were also obtained from the Agustín Codazzi Geographic Institute (IGAC). Table 1 presents the list of extraction wells selected for this study, which includes data about the dynamic level, static level, flow rates delivered to the water distribution company, and volume supplied. Additionally, static level and water table data were obtained from wells 44-IV-D-PZ-02, 44-IV-D-PZ-04, 44-IV-D-PZ-22, 44-IV-D-PZ-01A, 44-IV-C-PZ-01A, 44-IV-C-PZ-01B, and 44-IV-B-PZ-02, which belong to the piezometric network used by CARSUCRE to monitor aquifer behaviour. The images used for the land cover and land use analysis study were downloaded from the United States Geological Survey (USGS) through the Earth Explorer website (https://earthexplorer.usgs.gov/) for the years 2017, 2020, and 2023 during the two well-defined seasons in the study region: summer (January and February) and winter (September and October). This allowed for comparing vegetation cover at different times of the year. Finally, data from GRACE-Geovanni, a web application from the Goddard Earth Sciences Data and Information Services Center (GES DISC), Distributed Active Archive Center (DAAC) of NASA, and the Jet Propulsion Laboratory (JPL) were used to assess the water storage capacity of the Morroa aquifer [39]. The GRACE missions provide detailed measurements of Earth's gravitational field changes, relating them to underground water content, offering data from 2002 to 2015. Since then, the GRACE-FO mission has provided the required data [40].

Table 1. Wells monitored in the present study.

Identification	Number Well	Location	Flow Rate Delivered (lt/s)
44-IV-D-PP-31	32	Corozal	20
44-IV-D-PP-35	36	Corozal	25
44-IV-D-PP-38	02	Corozal	45
44-IV-D-PP-37	01	Corozal	45
44-IV-D-PP-42	03	Corozal	35
44-IV-D-PP-43	43B	Corozal	18
44-IV-D-PP-44	45	Corozal	20
44-IV-D-PP-46	46	Corozal	120
44-IV-D-PP-47	47	Betulia	100
44-IV-D-PP-48	48B	Los Palmitos	80
44-IV-D-PP-51	51	Los Palmitos	60
44-IV-D-PP-16	40	Corozal	14
44-IV-D-PP-01	35	Corozal	35

2.3. Methodology

This research is divided into two fundamental parts, knowing that DT is a virtual model replicating the implementation of a physical object [41]. The first part details all the elements related to the virtual model of the DT, breaking it down into five layers of information that interact with each other, feeding the proposed structure, and generating real scenarios based on historical and present data, which are described below. The second part addresses the proposed physical object for the DT, which is implemented through a wireless sensor network (WSN) deployed in the study area. Finally, both models utilise an objective function (OF) specifically designed to enable optimal system control [42]. This control approach serves as the foundation for a decision-support platform to manage water resources efficiently. The subsequent sections describe each of the proposed stages for the DT.

2.3.1. Hydrogeological Stage

The first stage of the model corresponds to the hydrogeological component, which forms the physical and conceptual foundation of the aquifer's digital twin. This stage integrates historical data on static and dynamic levels from monitoring wells and extraction data, enabling the characterisation of aquifer dynamics and its response to different scenarios involving anthropogenic pressures and climatic variability. Additionally, orographic, edaphic, and hydrological variables related to the Morroa aquifer system and its recharge area are incorporated, sourced from official databases such as CARSUCRE, IDEAM, IGAC, and the Government of Sucre. This information is complemented by findings from recent technical studies, notably the Environmental Hydrological Model of the Morroa Aquifer (Convenio 036/2013 of the General System of Royalties) [38], conducted between 2012 and 2017. The integration of these datasets provides a detailed perspective on the geospatial, geological, morphometric, and hydrological aspects of the aquifer, facilitating a comprehensive understanding of its behaviour as a complex underground system.

Within this component, a conceptual model of the aquifer system was developed, integrating its geometry [43], boundaries [44], hydraulic properties [45], and hydrochemical characteristics [46]. Additionally, the model encompasses the spatial and temporal distribution of recharge, discharge, and extraction processes and the directions and magnitudes of groundwater flow [47].

2.3.2. Remote Sensing

The second stage corresponds to the remote sensing layer, which integrates multitemporal satellite imagery acquired from sensors aboard various orbital platforms, exhibiting different spatial and temporal resolutions. This layer enables dynamic characterisation of the aquifer's surface environment through digital image processing using advanced algorithms for supervised classification, spectral analysis, and change detection. Image processing facilitates monitoring critical variables such as LULC, vegetation indices, soil moisture, and potential recharge areas. Additionally, it allows for the indirect observation of patterns potentially related to overexploitation processes, such as decreased vegetation cover or the expansion of intensive agricultural activities in critical zones. This information is essential to establish connections between surface dynamics and the evolution of the underlying aquifer, particularly in regions with limited availability of in situ data. Figure 4 illustrates the methodological workflow employed in this stage, detailing the process from image acquisition to the generation of thematic layers, subsequently integrated into the overarching Digital Twin model.

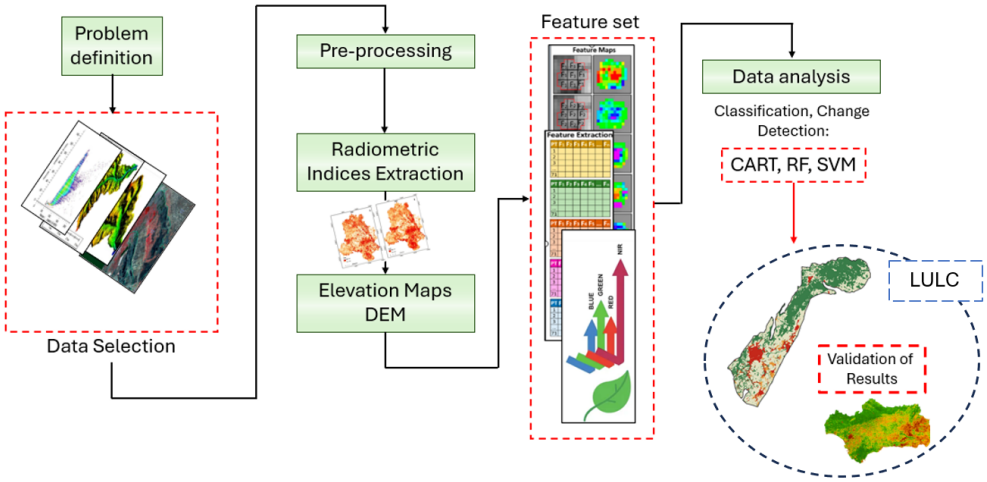

Figure 4. Methodological steps for land use and land cover classification from satellite data.

Considering the resilience model proposed from the DT in this study, the remote sensing stage was used with two primary objectives: to establish the classification of the aquifer coverage area and to define LULC to understand the dynamics of the variables that can affect aquifer levels and their recharge processes (such as population growth, reduction of surface water sources, reduction of forests and thick vegetation, and climate change). For Sentinel-2 images, bands 2 (blue), 3 (green), 4 (red), and 8 (Near-infrared or NIR) with a spatial resolution of 10 m were selected [14,15], whereas MODIS images with spatial resolutions of 500 m and 1 km were used, specifically MODIS/NTSG/MOD16A2/105 [33,37]. Planet images with a 3 m spatial resolution were used for land use and land cover classification studies. Additionally, data from sound level sensors, piezometers, and historical data provided by Carsucre were integrated to validate satellite imagery, complement statistical analyses, and estimate the necessary correlations.

Preprocessing included radiometric and atmospheric corrections (TOA), filtering, and other techniques using specialised software such as QGIS version 3.26.2 Buenos Aires and ArcGIS version 10.8.2. Information extraction focused on three indices (NDVI, NDWI, and EVI) across six classes: surface water, urbanised areas, crops, bare soil, low vegetation, and high vegetation (forests). A total of 150 training and test samples were obtained for each class by photointerpretation. Data analysis tools such as the Google Earth Engine were used primarily for classification, implementing algorithms such as K-means, Random Forest, CART, and various statistical analyses [48]. The QGIS software was used to visualise the

resulting maps. Likewise, groundwater storage data were downloaded using the Band-K Microwave Range sensor from GRACE (NASA) [49], with a resolution of about 50 km, using the Giovanni web portal to be used in the resilience model as "Storage Capacity" of the aquifer over time [50]. The results of the satellite image processing were validated using historical well data distributed throughout the aquifer. The accuracy of these results was evaluated by experts from the Corporación Autónoma Regional (Carsucre), the governmental entity that has under its jurisdiction the supervision and management of the water resources of the Morroa Aquifer.

2.3.3. WSN Sensor Networks

For this stage of DT, a hybrid monitoring network is proposed, utilising a wireless sensor network (WSN) for real-time measurement of variables related to water quality, aquifer level, and flow, along with the development of software aimed at implementing early warning alerts as decision-making tools in aquifer management. This phase includes piezometers located in the recharge zone of the Cali Savannas, along with barometric sensors and wireless continuous measurement devices (Divers), completing a telemetric sensor network prototype controlled from a remote terminal (PC, Smartphone, Tablet) for real-time management and control of the aquifer extraction point. Additionally, for data acquisition and management of embedded systems, the proposed method involves using ESP32-type control cards, modular measurement amplifiers for the Internet of Things (PMX), and the Python (Version 3.13.3) programming language. Techniques for handling captured data are based on machine learning and deep learning to generalise behaviours from the supplied information and provide early warning for water resource management using tools such as Python and TensorFlow [51].

From this stage, to facilitate tasks and achieve an abstraction that allows any user to create interconnections, as well as to avoid problems related to technology management, the proposal suggests using domain-specific language (DSL) tools supported by model-driven engineering (MDE), so that IoT objects can offer the necessary algorithms in a simple and friendly manner [52].

The proposed model comprises nodes or motes deployed in various wells belonging to the CARSUCRE piezometric network. These nodes are interconnected and transmit data regarding water levels and quality using LoRa communication technology. The collected information is forwarded to a processing centre, where the acquired data are visualised and utilised to implement predictive algorithms and early warning systems, leveraging advanced data science techniques and artificial intelligence. This comprehensive approach ensures continuous and accurate aquifer monitoring, facilitating informed decision-making and enabling proactive measures for water resource management. The infrastructure of the Wireless Sensor Network (WSN), combined with sophisticated data processing capabilities, represents a powerful tool for the conservation and efficient management of the Morroa Aquifer [53].

2.3.4. Control and Optimisation

Once data from the hydrogeological, remote sensing, and in-situ sensor stages are consolidated, the control and optimisation module is developed, aiming for efficient and resilient groundwater resource management. This stage implements a simulation-optimisation model capable of predicting aquifer behaviour under various climatic stress scenarios by integrating mathematical modelling techniques, predictive control, and heuristic optimisation algorithms. Its primary objective is to dynamically adjust extraction strategies to maintain stable and sustainable operational conditions over time, ensuring system resilience against fluctuations in recharge and demand [42]. The model is struc-

tured upon a general water balance formulation, considering critical variables such as the piezometric water level $H(t)$, extraction rate Q_{out}, and recharge rate Q_{in} [54]. From these variables, an objective function (OF) guiding the optimisation process is defined. This function aims to minimise deviations of the actual water level from a target level H_{obj}, established by the competent environmental authority (CARSUCRE) for each monitored well (Table 1), while simultaneously keeping the system within technical and operational constraints.

The OF is formulated as a weighted combination of criteria: Firstly, minimising the mean squared error between $H(t)$ and H_{obj} and secondly, maximising efficiency in the relationship between Q_{out} and Q_{in} thus ensuring sustainable equilibrium. This approach facilitates evaluating various extraction configurations under multiple input conditions, identifying optimal extraction rates to preserve aquifer integrity and mitigate the risk of overexploitation [55].

$$\min \sum_{i=1}^{T} \left[\alpha (H_t - H_{obj})^2 + \beta \left(\frac{Q_{out,t}}{Q_{in,t}} \right) \right] \quad (1)$$

The weighting coefficients α and β adjust the relative balance between maintaining the water level and ensuring the sustainability of extraction. To determine the optimal values of these coefficients for implementation in the study area, three types of heuristic algorithms were employed: grid search, Genetic Algorithm (GA), and Particle Swarm Optimisation (PSO) [56]. These algorithms were individually integrated into a general hybrid algorithm that combined the results of the aforementioned heuristics with a controlled aquifer model to optimise the management of groundwater resources (1).

The quadratic term $(H_t - H_{obj})^2$ ensures that both the positive and negative deviations of H_t from H_{obj} are penalised equally, making the function more sensitive to large deviations and thus to significant errors. In contrast, the linear term $\frac{Q_{out,t}}{Q_{in,t}}$ provides a direct measure of flow balance. Maintaining a low ratio indicates that the extraction rate does not significantly exceed the amount of water recharged into the aquifer, reflecting an adequate and sustainable balance for this vital resource [57]. The model constraints [58] are defined in Appendix A.

2.3.5. Aquifer Resilience and Management Strategies

The final stage of the system corresponds to the aquifer resilience model, designed to evaluate its capacity for recovery from sustained external disturbances such as prolonged droughts, localised over-extraction, or unexpected increases in water demand. This model represents a strategic component of the DT, aimed at quantifying the system's operational stability under critical conditions and identifying thresholds beyond which the aquifer's response compromises its long-term sustainability.

In this stage, the DT consolidates results generated from hydrogeological, satellite, sensor-based, and optimisation layers, integrating them through a computational analysis architecture that enables dynamic assessment of aquifer performance under multivariable scenarios. Real-time simulation and visualisation tools monitor key variables such as static levels, recharge, and extraction rates, facilitating the detection of significant deviations from the reference conditions established by target levels (H_{obj}) for each well.

The system provides detailed information on current groundwater extraction rates, comparing them with optimal values derived from the control model and identifying cases where such deviations might trigger aquifer depletion or functional deterioration. Additionally, retrospective and prospective simulations under various climatic scenarios, including extreme precipitation events or prolonged droughts, are conducted. These

simulations help evaluate the structural and operational resilience of the aquifer, as well as the effectiveness of existing management strategies.

Based on these analyses, the DT acts as a decision-support tool for environmental authorities and water resource operators, providing quantitative evidence regarding the necessity for corrective measures or complementary actions, such as the redistribution of extraction loads, implementation of artificial recharge zones, or activation of contingency plans in response to extreme hydrological events. Collectively, this stage strengthens the system's ability to anticipate risks, adapt to changing conditions, and maintain hydrogeological balance in the medium and long term. Figure 5 provides an integrated overview of the proposed Digital-Twin-based approach for resilient management of confined aquifers, structured around five interconnected functional layers.

On the left side, the physical configuration of the field monitoring system is illustrated, consisting of an instrumented well equipped with water-level and quality sensors connected via LoRa technology to a weather station and a Wireless Sensor Network (WSN). This IoT infrastructure enables continuous acquisition of hydrological and environmental data from the aquifer, traversing various soil layers until reaching the confined water. The instrumentation is designed to operate in real-time, continuously feeding the DT model with data that accurately reflects the aquifer system's behaviour under various extraction and climatic conditions.

The data and processing layers comprising the Digital Twin are detailed on the right side. Ultimately, all these elements converge within an analytical and IoT platform, which feeds into a decision-support system targeted at environmental entities, facilitating adaptive and resilient groundwater resource management strategies.

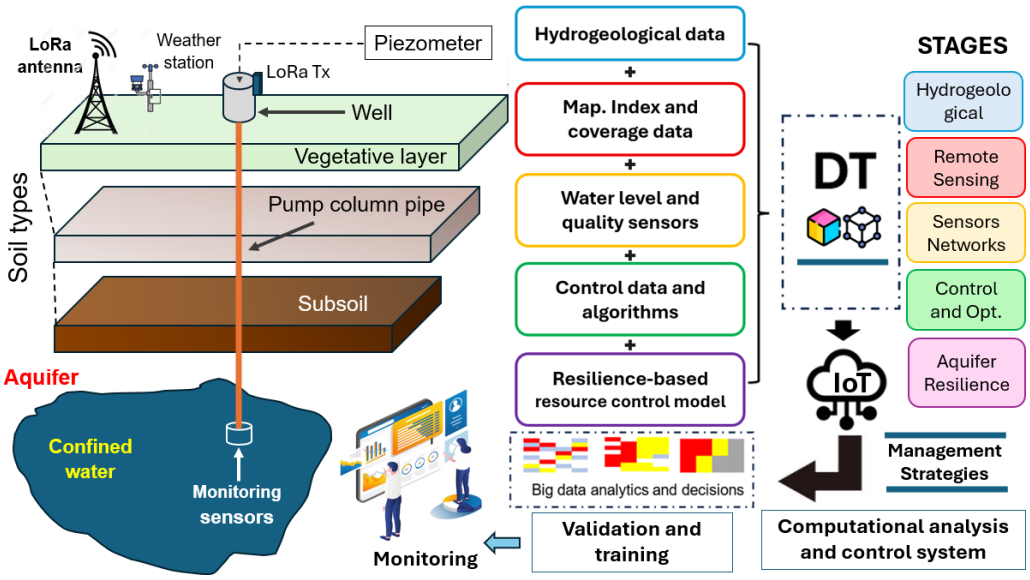

Figure 5. General architecture of the proposed IoT-DT platform for the Morroa aquifer.

3. Results

The proposed DT uses the confined Morroa aquifer in Colombia as a case study, where the primary critical variable is groundwater level—both static and dynamic [7,45,59,60]. Although the resilience model does not incorporate water quality variables, understanding the hydrogeological dynamics and behaviour of the system is essential for interpreting its historical evolution and anticipating future scenarios [61]. Due to the aquifer's structural complexity and geographical extent, a detailed characterisation is required to provide a solid foundation for the upper layers of the DT.

For this reason, the first layer of the digital twin is informed by meteorological records, historical monitoring well data, and satellite observations, as previously discussed. Specifically, it leverages the multilayer hydrogeological conceptual model developed by the Corporación Autónoma Regional de Sucre (CARSUCRE), illustrated in Figure 6a [59]. This model is complemented by a regional stratigraphic cross-section (Figure 6b) and a deep geological profile (Figure 6c), which together enable the interpretation of structural dynamics, lateral continuity, and subsurface flow behaviour within this highly complex confined aquifer [62].

Figure 6a illustrates the overall functioning of the system, in which groundwater is recharged in elevated areas through diffuse infiltration from the surface and then flows laterally under confined conditions toward discharge zones, following a hydraulic gradient governed by the regional geological structure. This system comprises multiple aquifer units separated by aquitards, generating both vertical and lateral heterogeneity. Figure 6b reinforces this conceptualisation by detailing the arrangement and dip of hydrostratigraphic units such as the Toluviejo Formation (T_{et}), El Carmén Formation (T_{mc}), and the adjacent lower and upper Sincelejo Formations (T_{psi} and T_{pss}), alongside aquifer levels A–E. These structural features provide a clearer view of the continuity of permeable strata and potential flow barriers.

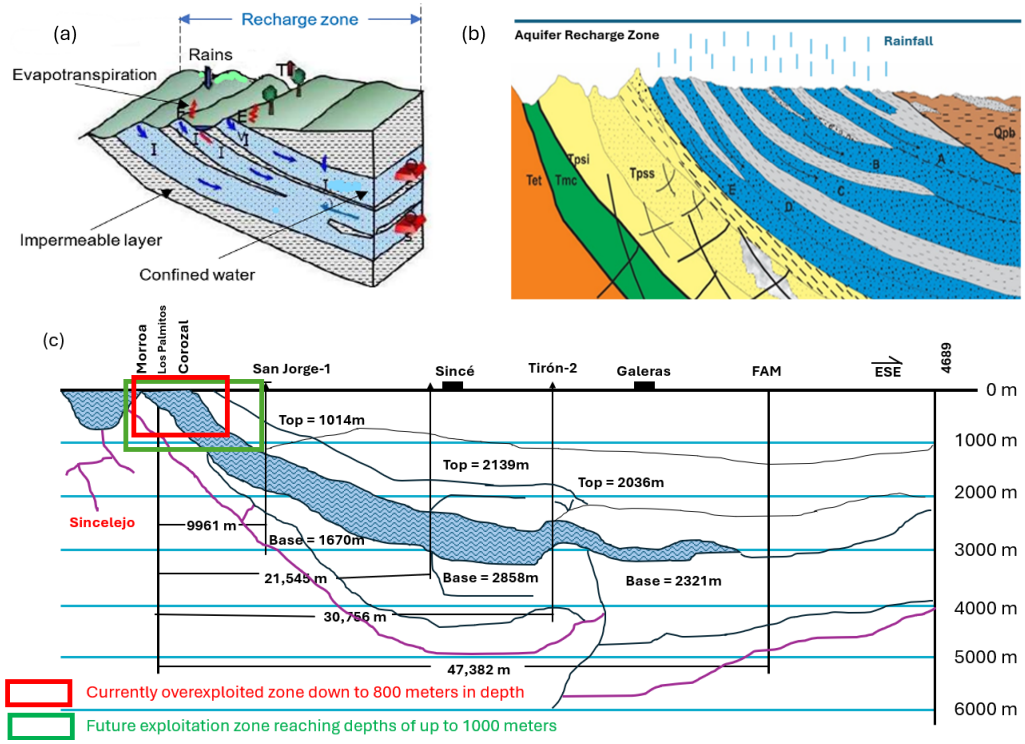

Figure 6. Conceptual hydrogeological model (**a**), Geological cross-section with the levels of the Morroa aquifer (**b**) and Geometry of the Morroa Aquifer (**c**) [59].

Figure 6c presents a regional geological profile extending over 47 km in an E-SE direction, spanning from the municipality of Morroa to Galeras and encompassing key locations such as Corozal, Los Palmitos, Sincé, and Sincelejo. This cross-section allows for a detailed examination of the deep geometry of the aquifer, whose principal units extend from approximately 1000 to 3000 m in depth. Two distinct zones of intensive groundwater extraction are clearly identified: (i) an overexploited zone (highlighted in red), located between Sincelejo, Morroa, Corozal, and Los Palmitos—areas of high population density—where wells have reached depths of up to 800 m; and (ii) an extraction zone extending to depths of approximately 1000 m (highlighted in green), which stretches

toward the San Jorge region. These areas exhibit a high density of wells and significant water demand, with a documented and progressive annual decline in piezometric levels.

According to data from CARSUCRE (2001–2022), the Morroa aquifer currently contains 113 active deep wells, 13 inactive ones, and 36 that have been abandoned, with depths ranging from 41 to 854 m. These wells extract groundwater at rates between 1 and 120 L per second, operating under an average pumping regime of 18 h per day, resulting in a total extraction rate of 1363 L per second. Static water levels in wells located in Sincelejo, Corozal, and Morroa range from 66 to 119 m deep, while dynamic pumping levels vary between 87 and 160 m. A reported average decline in static levels of between 1 and 3 m per year reflects the significant extraction pressure exerted on the aquifer. Lithologically, the Morroa aquifer is classified into four major groups: (1) the sandy-conglomeratic Morroa (levels A and B), (2) the sandy Morroa (levels C and D), (3) the sandy-clayey Morroa (levels E and F), and (4) the clayey Morroa (interbedded aquitards). Level A consists of fine- to coarse-grained lithic sandstones with conglomeratic lenses and clay layers [63]. It has high primary permeability and a structural configuration favourable for recharge, with thicknesses ranging from 30 to 226 m and dips of 5°–10° eastward. Level B, located beneath A and separated by a clay lens, contains friable sandstones and gravel layers, with thicknesses ranging from 38 to 164 m and dips of 10°–15°, also showing good permeability. Levels C and D, separated by clay layers, consist of fine sandstones, gravels, and occasional claystones, with thicknesses between 40 and 60 m. Finally, levels E and F comprise medium-grained sandstones, conglomeratic lenses, and intercalated clay layers ranging in thickness from 40 to 60 m. It is presumed that permeability decreases with depth due to compaction processes, which also affect water quality by increasing the concentration of dissolved ions and water temperature.

Generally, evapotranspiration in the area far exceeds precipitation, severely limiting direct aquifer recharge. This issue is further exacerbated by high surface runoff and intensive groundwater extraction. Other sources of recharge have been proposed, such as indirect infiltration from intermittent watercourses, leakage from improperly sealed abandoned wells, slow percolation from clay layers, and vertical transfer from the overlying Betulia Formation (Q_{pb}), as shown in Figure 6b. Moreover, it is hypothesised that intensive exploitation may induce downward recharge from deeper strata, which could explain the detection of groundwater ages as old as 5000 years in some samples ([59]).

Studies supported by the National Hydrocarbons Agency (ANH) [44], the Colombian Geological Survey (SGC) [64], and the Ministry of Environment and Sustainable Development (MADS) [65] confirm that the Morroa aquifer exhibits a monoclinal geometry that dips eastward, reaching depths greater than 3000 m (Figure 6c). This geological structure explains the absence of natural discharge from the system, as it is overlain by thick clay sediments that function as an effective vertical barrier [66]. Although the aquifer holds substantial reserves, most of them lie below 1000 m, where current extraction is not economically feasible. Furthermore, the lower sections of the aquifer have yet to be fully characterised in terms of their hydraulic properties and water quality [59]. This integrated characterisation—both geological and operational—provides the physical foundation upon which the DT of the Morroa aquifer is constructed. It will enable more accurate modelling of the system's dynamic behaviour and support decision-making processes aimed at achieving sustainable and resilient groundwater management.

In light of the above, this study analysed data from monitoring wells 04 and 75 as representative case examples. Despite being several kilometres apart, both wells are hydraulically connected within the uppermost unit, layer A (Figure 7a). This unit exhibits a thickness ranging from approximately 30 to 226 m. The hydraulic continuity between these points is influenced by the dip of the stratigraphic units—ranging between 5° and 10°

eastward [45]—which, when combined with Bernoulli's principle, facilitates the analysis of synchronous measurements across distant locations.

Thus, well 04 (coded 44-IV-D-PZ-04), equipped with a piezometer, measured the static level in well 75, which is an extraction well. In contrast, wells 02 and 11, as shown in Figure 7a, are not connected and therefore do not allow for comparative measurements. Based on this principle, the level data obtained in Figure 7b shows the behaviour of well 04 over the years, which is the information used to develop the proposed DT model. As shown in Figure 7b, the green rectangles indicate areas with missing data owing to erroneous measurements or a lack of historical data. Data imputation was applied using neural networks [67]. Furthermore, to remove noisy or extreme data, a Whittaker smoother (WS) with hyperparameter $\lambda = 0.2$ was used [68].

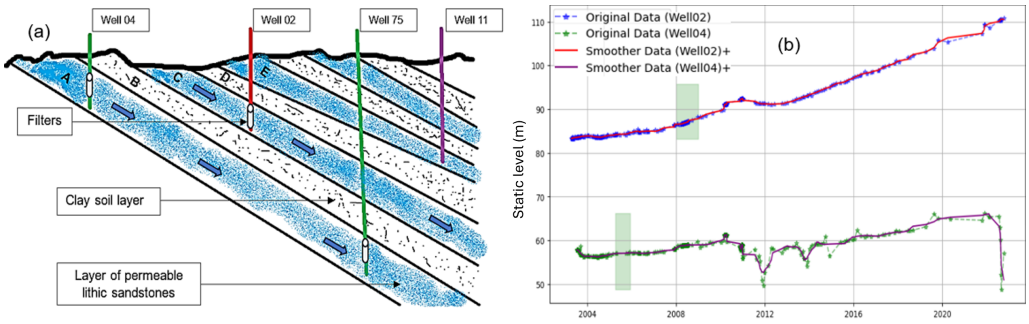

Figure 7. (**a**) Profiles of aquifer layers and location of well levels and (**b**) static levels in well 44-IV-D-PZ-04.

On the other hand, regarding LULC classification shown in Figure 8, multiple algorithms were implemented using the GEE platform and high-resolution imagery (3-meter spatial resolution) provided by Planet. Domain experts, including professionals from CARSUCRE, validated classification points. Among the tested approaches, the Random Forest machine learning algorithm yielded the most accurate results, achieving a Kappa coefficient of 0.8921 and an overall accuracy of 91.12%. This ensemble method constructs multiple decision trees, each trained on a randomly sampled subset of the input feature space with identical and independent distributions [69].

Figure 8 displays three LULC classification maps corresponding to the dry season (January) across the aquifer region for 2017, 2020, and 2023. These maps reveal a progressive decline in vegetative cover, likely attributable to increasingly arid conditions. For consistency, all maps were generated using data from the same month, ensuring valid temporal comparisons across land cover classes [70]. The identified classes include water bodies (blue), built-up areas (red), croplands (light green), bare or sparsely vegetated soils (ochre), medium-height grasslands (olive green), and dense vegetation or forests (dark green).

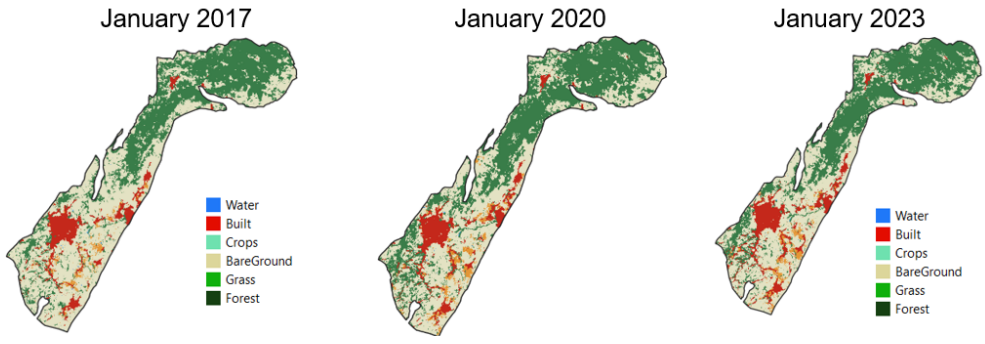

Figure 8. LULC classification maps 2017–2023.

The percentage values for each class defined using the Google Earth Engine platform [71] were complemented with historical data from the Agustín Codazzi Institute of Colombia. Comparing the obtained data (Figure 9), it was observed that the built-up area in hectares increased by approximately 40% compared with the year 2000. Additionally, the cultivated area between 2000 and 2023 saw an increase of 48%, whereas the area composed of forests or tall and dense crops decreased by 7% over the same period (Figure 9b). These three elements may contribute to the low resilience of the aquifer in question. Expanding the built-up area implies that the population dependent on aquifers continues to grow. Coupled with the fact that agriculture, one of the largest water consumers, is expanding and the forested area is shrinking, it becomes clear that the vegetation cover has been increasingly compromised, thus contributing less to the aquifer's recharge.

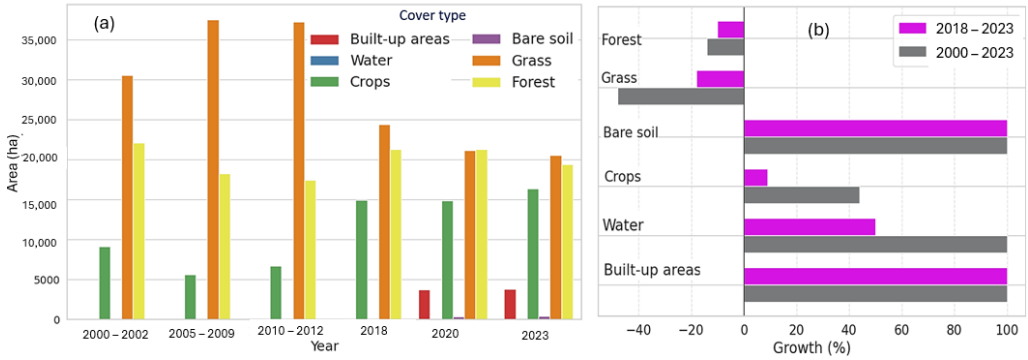

Figure 9. (**a**) Distribution in hectares of land cover classes present in the Morroa aquifer area from 2000 to 2023. (**b**) Gain or loss factor for each class.

Proof. Proposed DT in the Study Area. The proposed DT is a hybrid approach system, as it integrates mechanistic methodologies based on physical models with data-driven strategies that leverage real-time data. This fusion enables a more accurate and dynamic representation of the aquifer by combining theoretical knowledge with continuously updated empirical information. Moreover, according to the service level scale of DT, the proposed model is classified as a prescriptive DT. This means that it not only forecasts future states or performance—including the remaining useful life of the aquifer and its components—but also recommends specific actions based on these predictions, thereby enhancing decision-making processes [24,72].

Figure 5 illustrates the general architecture of the proposed IoT–DT system. This system synergistically integrates multiple sources of previously described information—including hydrogeological data, satellite imagery, water level and quality measurements, and sensor data collected from strategically distributed IoT nodes across the aquifer—all consolidated through a robust IoT platform. Based on these inputs, the DT constructs a virtual representation of the aquifer system and its sensor network, enabling continuous, real-time monitoring of critical variables.

The model leverages advanced artificial intelligence, machine learning techniques, computational optimisation, and bio-inspired algorithms to calibrate the system optimally and predict future behaviours. This allows for estimating optimal water levels for each well, maximum allowable extraction flows, and water quality parameters, while also generating early warnings regarding potential risks such as overexploitation or contamination. In addition, the system incorporates optimal control algorithms that support decision-making under dynamic and complex scenarios. Finally, the training and validation process actively involves experts and end users, who contribute contextual knowledge and validate the accuracy of the generated models. This interaction ensures not only the system's reliability but also its ability to adapt to specific local conditions. The platform is envisioned as an

interactive environment for data-driven analysis, simulation, and developing strategic water management actions, thereby promoting resilient and efficient aquifer governance.

More specifically, the proposed DT would consist of a network of water level and quality sensors installed across various wells within the existing piezometric network of the Morroa aquifer (red points). It is important to note that the highlighted blue area represents the ROI, as illustrated in Figure 10a. These monitoring wells are located on the outskirts of the central municipalities that rely on reservoirs (green circles). Level and water quality sensors were installed within these wells, whose static levels ranged between 50 and 110 m in depth. These sensors transmit data through wired connections from the bottom of the well to the surface (Figure 10) using fibre-optic cables connected to a local LoRa transmitter (green rectangles). This transmitter is linked to an antenna between 3 and 4 km from the selected evaluation wells. The ID Tolú Technology Centre (a collaborative entity in the project) manages the antenna and sends this data to the collection centre. Implementing Internet of Things (IoT) tools creates a database for variables such as water level, dissolved oxygen, pH, conductivity, and temperature, with sampling intervals of 2–5 min (because the physical variables do not undergo significant instantaneous changes). This setup allows for the application of artificial intelligence algorithms not only to understand the current behaviour of the aquifer but also to predict its behaviour in the coming years under the current scenario and various simulated scenarios. □

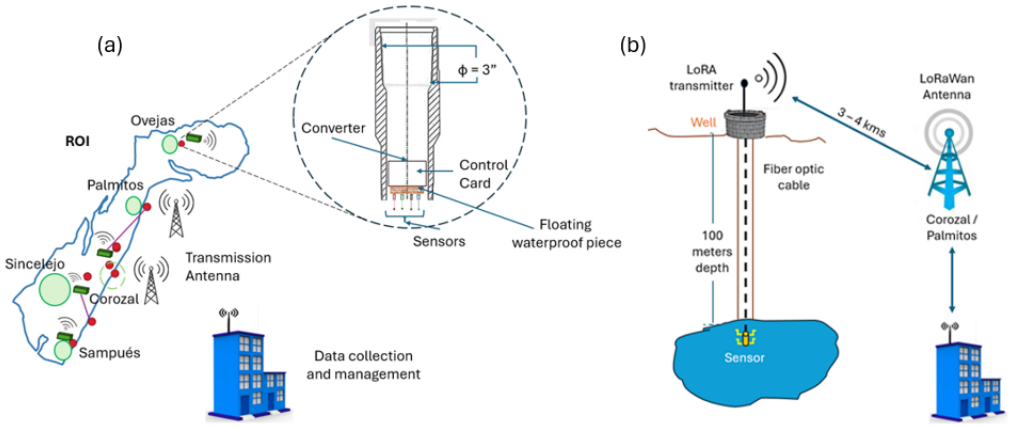

Figure 10. (**a**) Proposed DT design in the study area and (**b**) prototype implemented as a pilot test of the proposed DT.

Note that all activated nodes form a WSN, which provides real-time data from each well and is centralised through the cloud. This enables the rapid and efficient deployment of vital information related to aquifer recharge and most importantly, the contamination levels in the monitored wells. Consequently, regulatory agencies can implement management and conservation strategies for these reservoirs to ensure their sustainability over time.

Proof. DT Prototype in the Study Area. The following section describes the implementation of the first DT prototype in the study area. The most overexploited recharge zone, located at 9°21′31″ N–75°17′35″ W, 3 km northeast of the municipality of Morroa, in the district of Sabanas de Cali, on a property managed by Carsucre, was selected. This location was chosen because of its proximity to the region's two main cities, implying greater water resource exploitation. According to Figure 10 and the arrangement of the wells, Wells 04 (measurement well) and 75 (extraction well) were selected to feed the proposed model. The climatic data are presented in Figures 2 and 3 were used to feed models (A3), (A4), and (A5); subsequently, Qin(t) was determined using model (A6).

Regarding the information measured in the well, the data transmission device configuration was carried out using a LoRa 32 Heltec Automation module installed in well

04 of the Morroa Aquifer (Figure 10). The measurements were conducted using various electronic devices, including DS18B20 temperature sensors, an analogue pH sensor SKU SEN0161, a conductivity sensor SKU DFR0300, and a dissolved oxygen sensor in water SEN0237-A. These devices were lowered into the well using a 3-inch diameter sensor holder (Figure 10a). The conductivity and pH sensors were previously calibrated in the chemistry laboratory of the Corporación Universitaria del Caribe – CECAR, using water samples extracted from the well and recorded through the Sparklink PS-011 interface. This interface has Bluetooth ports and specific ports for Passport-type adapters through which the pH, temperature, and conductivity sensors are connected. Transmitting these data did not present significant difficulties related to packet transmission and sampling times, as the measured variables did not exhibit drastic changes in short periods. Therefore, the transmission sampling frequency used was 0.5 and 1 min, and the working frequency for transmission was 928 MHz. The transmission node was connected to a dissolved oxygen sensor in water, SEN0237-A, for data acquisition using a 32-bit ESP32 board powered by batteries. These tests are ongoing, and their results are visualised through an ID Tolú Technology Centre dashboard.

For this prototype, the control model used to determine the optimal exploitation levels in the wells was parameterized with an area of 10,000 m^2 (one hectare in the recharge zone), a hydraulic conductivity of 0.36 m/day (converted to 131.4 m/year), and a storage coefficient (S) of 0.0001 [63]. Recharge was estimated considering an LULC factor of 0.3 [73] and an annual recharge rate of 3% of the average precipitation [63]. An extraction (Qout) constraint of 20 litres per second was imposed, as this has historically been the exploitation value assigned to well 45 (Table 1) by the government authority to the regional water distribution company.

Optimisation of Parameters and DT Results: Table 2 presents the heuristics applied to find the best combination of parameters w_1 and w_2 in Equation (1). The PSO algorithm effectively minimises the root-mean-square error (RMSE) between the simulated and observed levels in (1). This algorithm uses a dataset covering 2000 to 2020, incorporating 21 years of time-series data on annual precipitation, evapotranspiration, and piezometric levels. The PSO hyperparameters were configured with the values c_1 = 2.05, c_2 = 2, and w = 0.8 [74]. Here, c_1 and c_2 represent the cognitive and social acceleration coefficients, respectively, and w is the inertia weight. These values were selected to balance the global exploration and local exploitation within the search space.

The results obtained with the DT prototype, using optimal control applied to the piezometric levels of an aquifer and optimised via PSO, are shown in Figure 11a. PSO determined the optimal weights $w_1 = 0.353$ and $w_2 = 0.647$ for the objective function, balancing the deviation of the piezometric level and the sustainability of the extraction. The blue line in the figure represents the simulated levels, which show a stable trend close to the target level set at 58.5 m (dotted green line), whereas the red line with markers shows the observed levels. The RMSE of 2.6158 m indicated a moderate discrepancy between the simulated and observed values. Notably, the optimised model maintained the simulated levels more steadily than the observed levels, especially in recent years, when the observed levels showed a significant increase. The lower graph of optimal annual extraction reveals how the algorithm dynamically adjusts extraction to maintain piezometric levels near the target, demonstrating the ability of PSO to generate an adaptive management strategy that seeks to balance resource exploitation with long-term preservation of the aquifer. □

Table 2. Heuristic methods applied to determine the optimal combination of hyperparameters for the control model's objective function applied to the Morroa aquifer's Test area.

Heuristic	Hyperparameters	Optimal Parameters for w_1 and w_2 in the OF	Average Optimal Q_{out}	RMSE, σ
Grid Search	Grid resolution of 21 × 21	0.297 and 0.703	9.34 L/s	3.3127
Genetic Algorithm (GA)	Population size	50	9.23 L/s	3.21 3.13 L/s
	Number of Generations	50		
	Crossover probability	0.7		
	Mutation probability	0.2		
	α (blend crossover)	0.5		
	μ	0.01		
	σ	0.2		
	Mutation probability per generation (%)	20		
Particle Swarm Optimisation (PSO)	Number of particles	50	8.3 L/s	2.61 2.82 L/s
	Number of iterations	100		
	Cognitive coefficient (c_1)	2.05		
	Social coefficient (c_2)	2		
	Inertia weight	0.8		

Optimisation and Forecasts of Groundwater Extraction: Figure 11b presents the results of the optimal groundwater extraction control obtained through PSO. The blue line shows the optimal annual extraction in litres per second (L/s) calculated by the model, whereas the red dotted line indicates the maximum extraction limit set at 20 L/s. PSO has developed an extraction strategy that adapts significantly over the study period (2000–2020) by adjusting to the changing conditions of the aquifer and hydrometeorological variables. The optimal extraction trajectory varies between approximately 4 and 14 L/s, demonstrating the ability of the algorithm to dynamically adjust the extraction in response to fluctuations in recharge and the piezometric level of the aquifer. In particular, the extraction remained consistently below the maximum limit, suggesting that the model achieves a balance between maximising the use of water resources and ensuring the long-term sustainability of the aquifer (resilience) [75,76].

Figure 11c illustrates different scenarios for the recharge area of well 04, simulating the well's behaviour in terms of its optimal extraction under various conditions: the La Niña phenomenon ($R_{anual} = 0.4$), El Niño phenomenon ($R_{anual} = 0.01$), seasons of hefty rainfall ($R_{anual} = 0.4$), and typical seasons ($R_{anual} = 0.03$). The results for these scenarios are as follows.

- R_{anual} at 1% and 3% (blue and cyan): Show the highest levels of optimal extraction, indicating that with low recharge rates, greater extraction is allowed to maintain the aquifer's target level.
- R_{anual} at 10% (green): Shows moderate extraction levels, generally lower than the 1% and 3% cases.
- R_{anual} at 40% (red): Presents the lowest levels of optimal extraction, suggesting that with a high natural recharge rate, less artificial extraction is needed to maintain the aquifer level.

Additionally, the figure shows notable temporal variations, with peaks around 2015 for all scenarios, which could indicate periods of higher water availability or lower demand. Significant drops in optimal extraction were observed around 2010 and 2017–2018 for all scenarios due to drought periods. A neural network LSTM model with a bootstrapping approach was employed to forecast for the next five years, as shown in Figure 11c. The LSTM model consists of three main layers: two LSTM layers, followed by a dense layer. The first layer has 50 units and returns sequences, whereas the second layer, which also has 50 units, does not. The output layer is dense with a single neuron for the final prediction. The model

was trained using the Adam optimiser and the MSE loss function over 100 epochs. The input data were normalised using MinMaxScaler and organised into sequences of 3-time steps. Training was conducted with historical data smoothed using the Whittaker filter ($\lambda = 0.315$). This relatively simple structure is ideal for capturing complex patterns in aquifer water extraction time-series data.

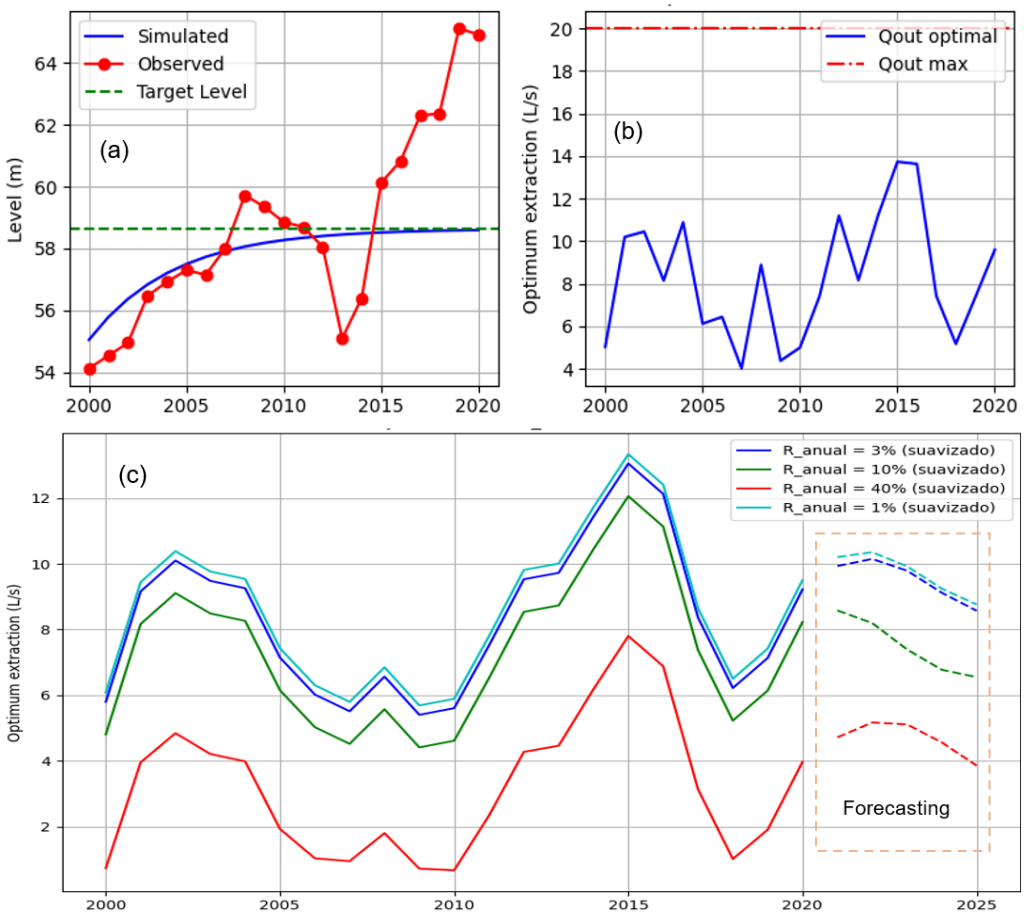

Figure 11. Results of the control algorithm (**a**), optimal values to maintain the target level (**b**), and simulated scenarios based on infiltration values and five-year predictions (**c**).

It is important to emphasise that, in the specific case of the Morroa aquifer, the current rate of exploitation is so high relative to its natural recharge that some experts have referred to it as a form of *"water mining"* [43]. This scenario implies that previously observed piezometric levels are unlikely to be restored under existing conditions. Therefore, even with the implementation of advanced technical strategies provided by the proposed DT, additional governmental policies would be essential to ensure the long-term sustainability of the aquifer system.

4. Discussion

This study proposed a methodology for implementing a hybrid and prescriptive DT, integrating mechanistic approaches based on physical models with data-driven strategies fuelled by real-time data streams. This combination enables a more accurate and dynamic representation of the aquifer system and the formulation of specific recommendations based on predictive insights. One of the main challenges addressed was deploying the IoT platform in a region with little to no existing communication infrastructure. In this context, LoRa technology emerged as one of the most viable and efficient options available, aligning with findings reported in previous studies ([77–81]). Regarding the hydrogeological

layer, the available information was highly complex, temporally dynamic, and spatially fragmented—factors that considerably increase the difficulty of modelling and integrating the system into advanced monitoring architectures such as the one proposed here.

To tackle this complexity, the authors advocate using IA, ML, and data-driven modelling tools to estimate key variables such as infiltration rates, recharge velocity, storage capacity, adequate precipitation, and evapotranspiration [23,76,82]. These variables directly impact the hydrodynamic behaviour of the aquifer, and their accurate modelling is essential for sustainable groundwater management [83,84]. In this regard, the digitalisation of hydrological models through emerging technologies represents a promising avenue for enhancing decision-making processes in global groundwater governance [25,85].

An additional operational limitation was identified: the service life of sensors deployed in deep wells is relatively short—ranging from 4 to 6 months—likely due to the high hydrostatic pressures involved. This results in recurring maintenance and replacement costs. Therefore, it is recommended to consider the integration of more robust and durable multiparameter sensors such as the Keller Series 36XiW-CTD, YSI EXO1/EXO2 Multiparameter Sonde, or In-Situ Aqua TROLL 500/600, which may help extend maintenance intervals and improve system reliability [86–88].

The findings of this study reinforce the value of integrating predictive models and optimisation algorithms into the resilient management of aquifers. Formulating an objective function based on the water balance equation—optimised using PSO and complemented by Whittaker smoothing and LSTM neural networks—enabled the anticipation of system behaviour under various climate scenarios [89]. Results show that the currently authorised extraction rates are unsustainable, even under favourable rainfall conditions. This highlights the urgent need for adaptive systems like digital twins to support informed, dynamic decision-making in groundwater resource governance [42,88,90].

5. Conclusions

This study presents a comprehensive approach for modelling and implementing a Digital Twin (DT) applied to a confined aquifer, integrating hydrogeological, climatic, real-time sensor data, and satellite imagery. A resilience-based control model was developed using the water balance equation to define an objective function, optimised through heuristic algorithms (Grid Search, GA, and PSO). PSO yielded the best performance (RMSE = 2.6158). The DT was deployed at a strategically selected well within the CARSUCRE piezometric network, following a five-layer architecture that defined a target water level of 58.5 m. Additionally, Whittaker smoothing and LSTM networks were incorporated to forecast the well's behaviour under various climatic scenarios. Results revealed that the licensed extraction rate (20 L/s) is unsustainable and that an optimal withdrawal rate of 8.3 L/s would be more appropriate to maintain the desired aquifer level.

As future work, the integration of real-time water quality data (pH, dissolved oxygen, temperature) is proposed, along with the deployment of Aquatrol 500/700 sensors across the piezometric network. This would enhance the DT's capabilities, supporting more innovative, adaptive, and sustainable groundwater management.

Given that the present study focused on monitoring and controlling the one-dimensional dynamics of the piezometric level in the Morroa aquifer—as this is its most critical and sensitive variable—a key priority for subsequent phases of the DT is the inclusion of additional groundwater quality parameters. Incorporating such variables will not only reinforce the robustness of the current model but also improve its predictive accuracy and broaden its scope, enabling integrated decision-making that accounts for both the quantity and the suitability of the groundwater resource.

Author Contributions: Supervision, conceptualisation, formal analysis, writing—original draft, C.S.C.-M.; conceptualisation, investigation, writing—original draft preparation, J.L.V.-R.; investigation, formal analysis, writing—review and editing, S.C.-L.; writing—review, investigation and editing, Y.T.S.-C.; validation, supervision, A.A.A.-M., conceptualisation, validation, supervision, O.E.C.-H. All authors have read and agreed to the published version of the manuscript.

Funding: This research received no external funding.

Data Availability Statement: The original contributions presented in this study are included in the article. Further inquiries can be directed to the corresponding author.

Acknowledgments: The authors express their sincere gratitude for the valuable technical and administrative support provided by the Corporación Universitaria del Caribe (CECAR) and its Vatio Laboratory, the Regional Environmental Authority of Sucre (CARSUCRE), and the Microrobotics Laboratory at Tecnológico de Monterrey (Mexico). Appreciation is also extended to the Doctoral Program in Engineering at Universidad Tecnológica de Bolívar and Universidad de Cartagena. In particular, the authors are grateful to the Ministry of Science, Technology and Innovation of Colombia (MinCiencias) and its Bicentenario II program for supporting the doctoral training of Colombian professionals. The authors also wish to express their gratitude to the Research and Development Laboratory of Tolú (ID Tolú), whose valuable collaboration was instrumental to the successful execution of this project.

Conflicts of Interest: The authors declare no conflicts of interest. The funders had no role in the study's design; in the collection, analyses, or interpretation of data; in the writing of the manuscript; or in the decision to publish the results.

Abbreviations

The following abbreviations are used in this manuscript:

NDVI	Normalised Difference Vegetation Index
NDWI	Normalised Difference Water Index
EVI	Enhanced Vegetation Index
ROI	Region of Interest
IGAC	Instituto Geográfico Agustín Codazzi (Colombia)
IDEAM	Instituto de Hidrología, Meteorología y Estudios Ambientales (Colombia)
LORA Tx	Long Range Transmitter
PSO	Particle Swarm Optimisation
AG	Directory of open access journals
LULC	Land Use and Land Cover
MPC	Model Predictive Control

Appendix A

As a complement to the main model described in the article, a simplified mathematical formulation is presented below, which serves as the basis for the simulation–optimisation module of the DT. This equation provides a dynamic representation of the evolution of the aquifer's piezometric level under variable recharge and extraction conditions. Although it adopts a unidimensional approach, it constitutes a robust starting point for implementing predictive control strategies to ensure the sustainability of groundwater resources. Based on Equation (1), and using the calibrated values of α and β shown in Table 2, the following is defined:

a. Water balance: The model ensures that the change in water level is due to the difference between recharge and extraction.

$$H_{t+1} = H_t + Q_{in,t} - Q_{out,t} \tag{A1}$$

Extraction limits:

$$0 \leq Q_{out,t} \leq Q_{out,max} \tag{A2}$$

b. Where $Q_{out,max}$ is the maximum sustainable extraction capacity determined in the previous studies.

c. Recharge (Q_{in}): Recharge is a function of precipitation P_t, land use and land cover $LULC_t$, and geological parameters K.

$$Q_{in,t} = f(P_t, LULC_t, K) \tag{A3}$$

To calculate the effective precipitation that contributes to recharge after considering evaporation and surface runoff,

$$P_{\text{efectiva}}(t) = P(t) - E(t) - R(t) \tag{A4}$$

where $E(t)$ is evaporation and $R(t)$ is surface runoff.
Geological parameters (K) include factors such as permeability (k) and porosity (ϕ), which affect the ability of the soil to transmit water.

$$K(x,y) = k(x,y) \cdot \phi(x,y) \tag{A5}$$

The contribution from all areas was then calculated to obtain the total recharge:

$$Q_{in} = \int_A [\alpha P_{\text{efectiva}}(t) LULC(x,y) K(x,y)] dA \tag{A6}$$

Recharge Equation (A6) is integrated into an objective function (1), enabling the DT to minimise the deviation of the water level from the target level and maximise the sustainability of the aquifer [61].

References

1. Karn, A.; Kumar, S. The Sustainable Development Goals: A Global Agenda for Transformative Change Towards a Sustainable World. In *New Paradigms of Sustainability in the Contemporary Era*; CSMFL Publications: Jagadhri, India, 2024; p. 70. Available online: https://books.csmflpublications.com/book-9788195732289/ (accessed on 24 June 2025).
2. Mohan, C.; Gleeson, T.; Forstner, T.; Famiglietti, J.S.; de Graaf, I. Quantifying Groundwater's Contribution to Regional Environmental-Flows in Diverse Hydrologic Landscapes. *Water Resour. Res.* **2023**, *59*, 6. [CrossRef]
3. du Plessis, A. Water resources from a global perspective. In *South Africa's Water Predicament: Freshwater's Unceasing Decline*; Springer International Publishing: Cham, Switzerland, 2023; pp. 1–25.
4. Biswas, A.K.; Tortajada, C. Groundwater: An unseen, overused, and unappreciated resource. *Int. J. Water Resour. Dev.* **2024**, *40*, 1–6. [CrossRef]
5. Sun, L.; Wang, X.; Wang, S.; Sun, W.; Wang, J.; Di, H. Experimental study on soil deformation caused by overexploitation of groundwater. *Water Environ. Res.* **2024**, *96*, e11111. [CrossRef] [PubMed]
6. Mialyk, O.; Schyns, J.F.; Booij, M.J.; Su, H.; Hogeboom, R.J.; Berger, M. Water footprints and crop water use of 175 individual crops for 1990–2019 simulated with a global crop model. *Sci. Data* **2024**, *11*, 206. [CrossRef]
7. Pérez, A.J.; Hurtado-Patiño, J.; Herrera, H.M.; Carvajal, A.F.; Pérez, M.L.; Gonzalez-Rojas, E.; Pérez-García, J. Assessing sub-regional water scarcity using the groundwater footprint. *Ecol. Indic.* **2019**, *96*, 32–39. [CrossRef]
8. Hera-Portillo, Á.D.L.; López-Gutiérrez, J.; Mayor, B.; López-Gunn, E.; Henriksen, H.J.; Gejl, R.N.; Martínez-Santos, P. An initial framework for understanding the resilience of aquifers to groundwater pumping. *Water* **2021**, *13*, 519. [CrossRef]
9. Kpegli, K.A.R.; Alassane, A.; van der Zee, S.E.; Boukari, M.; Mama, D. Development of a conceptual groundwater flow model using a combined hydrogeological, hydrochemical and isotopic approach: A case study from southern Benin. *J. Hydrol. Reg. Stud.* **2018**, *18*, 50–67. [CrossRef]
10. Yidana, S.M.; Dzikunoo, E.A.; Tetteh, J.D.; Mejida, R.A. Multiple Conceptual Model Approach for Assessing Groundwater Resources Sustainability Under Multiple Stresses. *Water Resour. Manag.* **2024**, *38*, 173–191. [CrossRef]
11. Atanacković, N.; Štrbački, J.; Živanović, V.; Davidović, J.; Gardijan, S.; Stojadinović, S. Hydrochemistry-Based Statistical Model for Sourcing Groundwater Inrush into Underground Mining Works: A Case Study in Eastern Serbia. *Mine Water Environ.* **2024**, *38*, 1–13. [CrossRef]

12. Cetina, M.; Taupin, J.D.; Gómez, S.; Patris, N. Hydrodynamic conceptual model of groundwater in the headwater of the Rio de Oro, Santander (Colombia) by geochemical and isotope tools. *Water Supply* **2020**, *20*, 1567–1579. [CrossRef]
13. Ying, Z.; Tetzlaff, D.; Freymueller, J.; Comte, J.C.; Goldhammer, T.; Schmidt, A.; Soulsby, C. Developing a conceptual model of groundwater–Surface water interactions in a drought sensitive lowland catchment using multi-proxy data. *J. Hydrol.* **2024**, *20*, 628–649. [CrossRef]
14. Mustaquim, S.M. Utilizing Remote Sensing Data and ArcGIS for Advanced Computational Analysis in Land Surface Temperature Modeling and Land Use Property Characterisation. *World J. Adv. Res. Rev.* **2024**, *21*, 1496–1507. [CrossRef]
15. Al-Kindi, K.M.; Al Nadhairi, R.; Al Akhzami, S. Dynamic Change in Normalised Vegetation Index (NDVI) from 2015 to 2021 in Dhofar, Southern Oman in Response to the Climate Change. *Agriculture* **2023**, *13*, 592. [CrossRef]
16. Bajany, D.M.; Zhang, L.; Xia, X. Model predictive control for water management and energy security in arid/semiarid regions. *J. Autom. Intell.* **2022**, *1*, 100001. [CrossRef]
17. Ramos, H.M.; Kuriqi, A.; Besharat, M.; Creaco, E.; Tasca, E.; Coronado-Hernández, O.E.; Iglesias-Rey, P. Smart Water Grids and Digital Twin for the Management of System Efficiency in Water Distribution Networks. *Water* **2023**, *15*, 1129. [CrossRef]
18. Li, W.; Ma, Z.; Li, J.; Li, Q.; Li, Y.; Yang, J. Digital twin smart water conservancy: Status, challenges, and prospects. *Water* **2024**, *16*, 2038. [CrossRef]
19. Rodríguez-Alonso, C.; Pena-Regueiro, I.; García, Ó. Digital Twin Platform for Water Treatment Plants Using Microservices Architecture. *Sensors* **2024**, *24*, 1568. [CrossRef]
20. Cavalieri, S.; Gambadoro, S. Digital Twin of a Water Supply System Using the Asset Administration Shell. *Sensors* **2024**, *24*, 1360. [CrossRef]
21. Giustolisi, O. Digital transition, digital twin and digital water: History, concepts and overview for the application to aqueducts. *Digit. Water* **2023**, *1*, 2313975. [CrossRef]
22. Singh, D.; Sharma, V. Proposing a digital twin-based sustainable water governance system for rural Indian villages. *Int. J. Inf. Technol.* **2025**, *1*, 628–649. [CrossRef]
23. Henriksen, H.J.; Schneider, R.; Koch, J.; Ondracek, M.; Troldborg, L.; Seidenfaden, I.K.; Stisen, S. A new digital twin for climate change adaptation, water management, and disaster risk reduction (HIP digital twin). *Water* **2022**, *15*, 25. [CrossRef]
24. Anker, C. Digital Twin Paradigms Towards Monitoring Insights for Deep Aquifer Pumps. Ph.D. Thesis, Stellenbosch University, Stellenbosch, South Africa, 2023.
25. Morales Ortega, L.R. A Digital Twin for Ground Water Table Monitoring. Master's Thesis, University of Twente, Enschede, The Netherlands, 2023.
26. Marshall, S.R.; Tran, T.N.D.; Tapas, M.R.; Nguyen, B.Q. Integrating artificial intelligence and machine learning in hydrological modeling for sustainable resource management. *Int. J. River Basin Manag.* **2025**, 1–17. [CrossRef]
27. Olaleye, O.; Akintola, O.; Jımoh, R.; Gbadebo, O.; Faloye, O. Review and Comparative Study of Hydrological Models for Rainfall-Runoff Modelling. *Int. J. Environ. Geoinform.* **2023**, *11*, 119–129. [CrossRef]
28. Navarro Mercado, J.L. Monitoreo de las Obras Piloto de Recarga Artificial en el Acuífero Morroa, Departamento de Sucre, Colombia. Bachelor's Thesis, Universidad Eafit, Antioquia, Colombia, 2020.
29. Instituto de Hidrología Meteorología y Estudios Ambientales (IDEAM). *Estudio Nacional del Agua 2022*; Instituto de Hidrología Meteorología y Estudios Ambientales (IDEAM): Bogotá, Colombia, 2023.
30. Duan, H.; Zhao, H.; Li, Q.; Xu, H.; Han, C. Estimation of Evapotranspiration Based on a Modified Penman–Monteith–Leuning Model Using Surface and Root Zone Soil Moisture. *Water* **2023**, *15*, 1418. [CrossRef]
31. Chirouze, J.; Boulet, G.; Jarlan, L.; Fieuzal, R.; Rodriguez, J.C.; Ezzahar, J.; Chehbouni, G. Intercomparison of four remote-sensing-based energy balance methods to retrieve surface evapotranspiration and water stress of irrigated fields in semi-arid climate. *Hydrol. Earth Syst. Sci.* **2014**, *18*, 1165–1188. [CrossRef]
32. Guerschman, J.P.; McVicar, T.R.; Vleeshower, J.; Van Niel, T.G.; Peña-Arancibia, J.L.; Chen, Y. Estimating actual evapotranspiration at field-to-continent scales by calibrating the CMRSET algorithm with MODIS, VIIRS, Landsat and Sentinel-2 data. *J. Hydrol.* **2022**, *11*, 206.
33. Mu, Q.; Zhao, M.; Running, S.W. MODIS Global Terrestrial Evapotranspiration (ET) Product (NASA MOD16A2/A3). *Algorithm Theor. Basis Doc. Collect.* **2013**, *5*, 600. Available online: https://eospso.nasa.gov/content/algorithm-theoretical-basis-documents (accessed on 25 February 2025).
34. Wang, C.; Liu, L.; Zhou, Y.; Liu, X.; Wu, J.; Tan, W.; Xiong, X. Comparison between satellite derived solar-induced chlorophyll fluorescence, NDVI and kndvi in detecting water stress for dense vegetation across southern China. *Remote. Sens.* **2013**, *16*, 1735. [CrossRef]
35. Anthony, T.; Kafy, A.A.; Hakeem, A.; Alsulamy, S.; Khedher, K.M.; Shohan, A. Spatial analysis of land cover changes for detecting environmental degradation and promoting sustainability in Abeokuta, South Nigeria. *Kuwait J. Sci.* **2024**, *51*, 100197. [CrossRef]

36. Adeyeri, O.E.; Folorunsho, A.H.; Ayegbusi, K.I.; Bobde, V.; Adeliyi, T.E.; Ndehedehe, C.E.; Akinsanola, A.A. Land surface dynamics and meteorological forcings modulate land surface temperature characteristics. *Sustain. Cities Soc.* **2024**, *101*, 105072. [CrossRef]
37. Xing, Z.; Li, Z.L.; Duan, S.B.; Liu, X.; Zheng, X.; Leng, P.; Shang, G. Estimation of Daily Mean Land Surface Temperature at Global Scale Using Pairs of Daytime and Nighttime MODIS Instantaneous Observations. *J. Photogramm. Remote. Sens.* **2021**, *178*, 51–67. [CrossRef]
38. Universidad Antonio Nariño (UAN). Modelo Hidrogeológico-Ambiental para el Departamento de Sucre. In *Convenio Sistema Nacional de Regalías 036/2013*; Universidad Antonio Nariño: Bogotá, Colombia, 2017.
39. Wahab, F.; Al-Abadi, A.; Al-Ozeer, A. Groundwater depletion and annual groundwater recharge estimation in Nineveh Plain, Northern Iraq using GRACE, GLDAS, and field data. Model. *Earth Syst. Environ.* **2025**, *11*, 117. [CrossRef]
40. Hasan, M.S.U.; Saif, M.M.; Ahmad, N.; Rai, A.K.; Khan, M.A.; Aldrees, A.; Yaseen, Z.M. Spatiotemporal analysis of future trends in terrestrial water storage anomalies at different climatic zones of India using GRACE/GRACE-FO. *Sustainability* **2023**, *15*, 1572. [CrossRef]
41. Abdullahi, I.; Longo, S.; Samie, M. Towards a Distributed Digital Twin Framework for Predictive Maintenance in Industrial Internet of Things (IIoT). *Sensors* **2024**, *24*, 2663. [CrossRef]
42. Bierkens, M.F.; van Beek, L.R.; Wanders, N. Gisser-Sánchez revisited: A model of optimal groundwater withdrawal under irrigation including surface–groundwater interaction. *J. Hydrol.* **2024**, *635*, 131145. [CrossRef]
43. Carsucre. Estudio Técnico del Acuífero Morroa. *Grupo Aguas* **2017**. Available online: https://carsucre.gov.co/wp-content/uploads/2019/01/ESTUDIOTECNICO_ACUIFERO-Morroa_Corregido_c.pdf (accessed on 10 February 2025)
44. Vergara, V. Manejo de suelos en el acuífero Morroa, Sucre, Colombia, alternativa para el desarrollo agrícola sostenible. *Rev. Colomb. Cienc. Anim. Recia* **2019**, *11*, 51–66. [CrossRef]
45. Pacheco, D.; Villegas, P. *Caracterización Hidráulica del Acuífero Morroa Utilizando Pruebas de Bombeo*; Universidad de Sucre: Sincelejo, Colombia, 2003; p. 100.
46. Rodelo Bejarano, G.; Argumedo Vivas, H. Caracterización Hidroquímica y Bacteriológica del Acuifero de Morroa en los Municipios de Sampués; Sincelejo, Morroa, Corozal y Los Palmitos en el departamento de Sucre . 2002. Available online: https://agris.fao.org/search/en/providers/124942/records/67122c0f7f591113e2a4c47c (accessed on 2 February 2025)
47. López Ramírez, S.E. Actualización del Modelo Numérico del Acuífero Morroa Utilizando Visual Modflow Flex. Available online: https://repositorio.uniandes.edu.co/entities/publication/23db7d3d-b189-478d-be67-1b6f104e88c5 (accessed on 2 February 2025).
48. Nazir, J.; Ali, M.; Sarwar, A.; Khan, S.; Rehman, K.; Fahim, B.; Iqbal, B. Delineation and validation of GIS-based groundwater potential zones under arid to semi-arid environment using multi-influence-factors approach. *Geol. Ecol. Landscapes* **2024**, *24*, 1–17. [CrossRef]
49. Chukwuka, A.V.; Adegboyegun, A.D.; Oluwale, F.V.; Oni, A.A.; Omogbemi, E.D.; Adeogun, A.O. Microplastic dynamics and risk projections in West African coastal areas: Developing a vulnerability index, adverse ecological pathways, and mitigation framework using remote-sensed oceanographic profiles. *Sci. Total Environ.* **2024**, *24*, 175963. [CrossRef]
50. Zowam, F.J.; Milewski, A.M. Groundwater Level Prediction Using Machine Learning and Geostatistical Interpolation Models. *Water* **2024**, *16*, 2771. [CrossRef]
51. Esposito, M.; Palma, L.; Belli, A.; Sabbatini, L.; Pierleoni, P. Recent advances in internet of things solutions for early warning systems: A review. *Sensors* **2022**, *22*, 2124. [CrossRef]
52. Michael, J.; Blankenbach, J.; Derksen, J.; Finklenburg, B.; Fuentes, R.; Gries, T.; Walther, G. Integrating models of civil structures in digital twins: State-of-the-Art and challenges. *J. Infrastruct. Intell. Resil.* **2024**, *26*, 100100. [CrossRef]
53. Kumar, R.; Saxena, A. Smart Water Management and Resource Conservation. In *Sustainable Smart Cities and the Future of Urban Development*; Global Scientific Publishing: Faridabad, India, 2025; pp. 235–262. [CrossRef]
54. Sajil Kumar, P.J.; Schneider, M.; Elango, L. The state-of-the-art estimation of groundwater recharge and water balance with a special emphasis on India: A critical review. *Sustainability* **2021**, *14*, 340. [CrossRef]
55. Hesamfar, F.; Ketabchi, H.; Ebadi, T. Simulation-based multi-objective optimisation framework for sustainable management of coastal aquifers in semi-arid regions. *J. Environ. Manag.* **2023**, *3382*, 117785. [CrossRef]
56. Sakamoto, S.; Nakamura, S.; Barolli, L.; Takizawa, M. A Comparison Study Between Cuckoo Search and Particle Swarm Optimisation Based Intelligent Systems for Optimisation of Mesh Routers in a Small-Scale WMN. In *International Conference on P2P, Parallel, Grid, Cloud and Internet Computing*; Springer Nature: San Benedetto del Tronto, Italy, 2024; pp. 121–132. [CrossRef]
57. Sahoo, S.; Singha, C.; Govind, A.; Sharma, P. Review of aquifer storage and recovery opportunities and challenges in India. *Environ. Earth Sci.* **2025**, *84*, 122. [CrossRef]
58. Saad, S.; Javadi, A.A.; Chugh, T.; Farmani, R. Optimal management of mixed hydraulic barriers in coastal aquifers using multi-objective Bayesian optimisation. *J. Hydrol.* **2022**, *612*, 128021. [CrossRef]
59. Carsucre. *Informe Técnico y de Seguimiento del acuífero Morroa*; MADS-Colombia: Sincelejo, Colombia, 2023.

60. Alvarez Cordero, A.A.; Schmalbach Amorocho, L.I. *Estudio Sobre la Disponibilidad a Pagar Por Mantener el uso del Agua Potable del Acuífero Morroa*; Universidad de Sucre: Sincelejo, Colombia, 2018.
61. Azizi, H.R.; Azizi, H. Development of an integrated multi-objective approach to formulate optimal harvesting policies with the aim of sustainable management of groundwater resources: Study area: Varamin Plain. *J. Hydroinform.* **2023**, *25*, 469-490. [CrossRef]
62. Khan, M.; Almazah, M.M.; Ellahi, A.; Niaz, R.; Al-Rezami, A.Y.; Zaman, B. Spatial interpolation of water quality index based on Ordinary kriging and Universal kriging. *Geomat. Nat. Hazards Risk* **2023**, *14*, 2190853. [CrossRef]
63. Carsucre. Informe de Gestión del Plan de Acción Institucional, PAI 2020–2023. 2022. Available online: https://carsucre.gov.co/wp-content/uploads/2023/03/INFORME-AVANCE-PAI-CARSUCRE-_31-DE-DICIEMBRE-2022_V3-MinAmbiente2.pdf (accessed on 14 February 2025)
64. IDEAM. Anexo 7. Aguas Subterráneas. Instituto de Hidrología, Meteorología y Estudios Ambientales (IDEAM). 2024. Available online: https://www.ideam.gov.co/sites/default/files/prensa/boletines/2024-08-23/anexo_7_aguas_subterraneas_0.pdf (accessed on 12 February 2025).
65. Diaz Baldovino, M. Análisis de la Dinámica de Los Niveles de Agua del Acuífero de Morroa Desde los Pozos Operados por la Empresa Veolia, Aguas de la Sabana SAESP. Sincelejo, Colombia. 2024. Available online: https://repositorio.unicordoba.edu.co/entities/publication/ca5b2005-d4ac-4e12-9e8f-3d18415c4699 (accessed on 1 February 2025).
66. Servicio Geológico Colombiano (SGC). Memoria Técnica del Mapa de Aguas Subterráneas del Departamento de Sucre en Escala 1:250,000. Exploración y Evaluación de Aguas Subterráneas. Ingeominas: Bogotá, Colombia. 2025. Available online: https://recordcenter.sgc.gov.co/B3/12006025002778/documento/pdf/0101027781101000.pdf (accessed on 13 February 2025).
67. Cohen Manrique, C.; Villa, J.L.; Month, A.A.; Velilla, G.P. Application of Artificial Intelligence Tools, Data Processing, and Analysis in the Forecasting of Level and Flow Variables in Wells with Little Data from the Morroa Aquifer. In *Workshop on Engineering Applications*; Springer Nature Switzerland: Cham, Switzerland, 2023; pp. 228–239.
68. Liang, J.; Ren, C.; Li, Y.; Yue, W.; Wei, Z.; Song, X.; Lin, X. Using enhanced gap-filling and Whittaker smoothing to reconstruct high spatiotemporal resolution NDVI time series based on Landsat 8, Sentinel-2, and MODIS imagery. *ISPRS Int. J.-Geo-Inf.* **2023**, *12*, 214. [CrossRef]
69. Zhang, T.; Su, J.; Xu, Z.; Luo, Y.; Li, J. Sentinel-2 satellite imagery for urban land cover classification by optimized random forest classifier. *Appl. Sci.* **2021**, *11*, 543. [CrossRef]
70. Sapitang, M.; Dullah, H.; Latif, S.D.; Ng, J.L.; Huang, Y.F.; Malek, M.B.A.; Ahmed, A.N. Application of Integrated Artificial Intelligence Geographical Information System in Managing Water Resources: A Review. *Remote. Sens. Appl. Soc. Environ.* **2024**, *35*, 101236. [CrossRef]
71. Cohen-Manrique, C.S.; Correa, Y.T.S.; Villa-Ramírez, J.L.; Alvarez-Month, A. Impact of land cover variations on the Morroa aquifer (Colombia) static and dynamic levels through remote sensing analysis. *Geospat. Inform. XIV* **2024**, *13037*, 19–27.
72. DNV. A204: Qualification and Assurance of Digital Twins. In *Recommended Practice DNV-RP-A204*; DNV: Oslo, Norway, 2021. Available online: https://www.dnv.com/energy/standards-guidelines/dnv-rp-a204-assurance-of-digital-twins/ (accessed on 9 February 2025).
73. Adhikari, R.K.; Mohanasundaram, S.; Srestha, S. Impacts of land-use changes on the groundwater recharge in the Ho Chi Minh city, Vietnam. *Environ. Res.* **2020**, *185*, 109440. [CrossRef] [PubMed]
74. Maghsoudi, R.; Javadi, S.; Shourian, M.; Golmohammadi, G. Determining the optimal aquifer exploitation under artificial recharge using the combination of numerical models and particle swarm optimisation. *Hydrology* **2023**, *10*, 100. [CrossRef]
75. Granata, F.; Di Nunno, F. Pathways for Hydrological Resilience: Strategies for Adaptation in a Changing Climate. *Earth Syst. Environ.* **2025**, *10*, 29. [CrossRef]
76. Morlot, M.; Rigon, R.; Formetta, G. Hydrological digital twin model of a large anthropized Italian alpine catchment: The Adige river basin. *J. Hydrol.* **2024**, *629*, 130587. [CrossRef]
77. Aliagas, C.; Pérez-Foguet, A.; Meseguer, R.; Millán, P.; Molina, C. A Low-Cost and Do-It-Yourself Device for Pumping Monitoring in Deep Aquifers. *Electronics* **2022**, *11*, 3788. [CrossRef]
78. Promput, S.; Maithomklang, S.; Panya-Isara, C. Design and analysis performance of IoT-based water quality monitoring system using LoRa technology. *TEM J.* **2023**, *12*, 29. [CrossRef]
79. Kombo, O.H.; Kumaran, S.; Bovim, A. Design and application of a low-cost, low-power, LoRa-GSM, IoT enabled system for monitoring of groundwater resources with energy harvesting integration. *IEEE Access* **2021**, *9*, 128417–128433. [CrossRef]
80. Jabbar, W.A.; Ting, T.M.; Hamidun, M.F.I.; Kamarudin, A.H.C.; Wu, W.; Sultan, J.; Ali, M.A. Development of LoRaWAN-based IoT system for water quality monitoring in rural areas. *Expert Syst. Appl.* **2024**, *242*, 122862. [CrossRef]
81. Truong, V.T.; Nayyar, A.; Lone, S.A. System performance of wireless sensor network using LoRa-Zigbee hybrid communication. *Comput. Mater. Contin.* **2021**, *68*, 1615–1635. [CrossRef]
82. CIMA Foundation. A Digital Twin for the Water Cycle. Available online: https://www.cimafoundation.org/en/news/a-digital-twin-for-the-water-cycle/ (accessed on 13 April 2025).

83. Brocca, L.; Barbetta, S.; Camici, S.; Ciabatta, L.; Dari, J.; Filippucci, P.; Massari, C.; Modanesi, S.; Tarpanelli, A.; Bonaccorsi, B.; et al. A Digital Twin of the terrestrial water cycle: A glimpse into the future through high-resolution Earth observations. *Front. Sci.* **2024**, *1*, 1190191. [CrossRef]
84. Alperen, C.I.; Artigue, G.; Kurtulus, B.; Pistre, S.; Johannet, A. A hydrological digital twin by artificial neural networks for flood simulation in Gardon de Sainte-Croix Basin, France. In *IOP Conf. Ser. Earth Environ. Sci.* **2021**, *906*, 012112. [CrossRef]
85. Reinecke, R.; Pianosi, F.; Wagener, T. How to use the impossible map–Considerations for a rigorous exploration of Digital Twins of the Earth. *Socio-Environ. Syst. Model.* **2024**, *6*, 18786. [CrossRef]
86. Ahmed, T.; Creedon, L.; Gharbia, S.S. Low-cost sensors for monitoring coastal climate hazards: A systematic review and meta-analysis. *Sensors* **2023**, *23*, 1717. [CrossRef]
87. Snazelle, T.T. *Field Comparison of Five in Situ Turbidity Sensors*; Report No. 2020-1123; U.S. Geological Survey: Reston, VA, USA, 2020.
88. Zamora, P.B.; Cabria, H.B.; Rodolfo, R.S.; Siringan, F.P.; Befus, K.M.; Cardenas, M.B. Enhanced submarine groundwater discharge and freshening of a subterranean estuary from rain. *J. Hydrol.* **2025**, *659*, 133253. [CrossRef]
89. Biazar, S.M.; Golmohammadi, G.; Nedhunuri, R.R.; Shaghaghi, S.; Mohammadi, K. Artificial Intelligence in Hydrology: Advancements in Soil, Water Resource Management, and Sustainable Development. *Sustainability* **2025**, *17*, 2250. [CrossRef]
90. Singha, C.; Sahoo, S.; Tinh, N.D.; Ditthakit, P.; Lu, Q.O.; El-Magd, S.A.; Swain, K C. Climate-resilient strategies for sustainable groundwater management in Mahanadi River basin of Eastern India. *Acta Geophys.* **2025**, *73*, 1891–1926. [CrossRef]